Electronic Journal of Structural Engineering

Original Article

Cite this: DOI:10.56748/ejse.24635

Received Date: 8 May 2024
Accepted Date: 23 December 2024

1443-9255
https://ejsei.com/ejse

Behavior of Ferrocement Beams using Fiber Glass Mesh and Sea Water

Mohamed Hatem[a,b*], Nader Mohamed[a], Khaled Samy [b], Mohamed Abdelrazik[a]
[a] Department of Civil Engineering, Faculty of Engineering, Al-Azhar University, Cairo, Egypt
[b] Department of Civil Engineering, Faculty of Engineering, Higher Institute for Engineering, 5th settlement, Cairo, Egypt
*Corresponding author: mohamedelserwy@azhar.edu.eg

Abstract

The current study aims to study the structural behavior of ferrocement beams using seawater to produce concrete beams that can be used as an alternative to conventional reinforced concrete beams. The formulated beams would have a high resistance to loads and cracking and would be more economical and environmentally friendly than traditional concrete beams. This research also aims to conserve freshwater by using seawater as a substitute in the concrete mix and curing process. The experimental work includes three groups of beams, The water-cement ratio and seawater content were varied in the concrete mix. Six concrete specimens with dimensions of 1600 mm * 300 mm * 150 mm were cast. All specimens were reinforced with fiber glass bars and fiberglass mesh. The fresh water in concrete mixing was varied and replaced with seawater. The curing water for the beams was also replaced with seawater. The reinforcement ratios were also varied in the specimens. In the first group, a ferrocement beam was cast as a reference using potable water for casting. In the second group, three beams were cast with different seawater contents in the concrete mix. In the third group, two ferrocement beams were cast with different seawater contents in the concrete mix and curing water. The cracking load, load-deflection curves, energy absorption capacity and cracking patterns have been investigated. The results showed that increasing the seawater content increased the concrete strength by 5% to 15% and the ultimate load increased by 5% to 47%.

Keywords

Ferrocement concrete, Green concrete, Fiber glass, Sea water

1. Introduction

Concrete is the most used building material around the world, and it consumes more than a billion tons of fresh water and with the spread of concrete use, more and more fresh water will be consumed. Studies have shown that more than half of the world's population may lack fresh water by 2025. The construction industry consumes a significant amount of freshwater, estimated at over 10 billion tons annually. In areas grappling with water shortages, often exacerbated by natural disasters, this freshwater use can be a major concern. Seawater, on the other hand, presents a viable alternative for mixing concrete. Forecasts predict a worrying trend – by 2050, 75% of the water needed for concrete will be required in regions already grappling with water scarcity. In the last few years, the construction industry's reliance on freshwater is a growing concern. Freshwater limitations and the environmental drawbacks of desalination are pushing the industry towards innovative solutions. Seawater, once considered unsuitable, is emerging as a viable alternative for mixing concrete. This shift has the potential to significantly reduce freshwater consumption in construction, paving the way for a more sustainable future.

Seawater accounts for about 96.5% of the world's accessible water, it presents a compelling alternative to freshwater for concrete production, particularly in coastal regions where freshwater resources are scarce. As a renewable resource, unlike freshwater which is generally considered nonrenewable, seawater offers a more sustainable long-term solution for concrete mixing.

The concrete structures are weakened when exposed to chemicals, causing them to deteriorate rapidly. This reduces their lifespan and necessitates costly repairs and maintenance. Chemical attack is also a major culprit behind steel corrosion in reinforced concrete. There are many solutions to this problem, one approach involves using concrete designed for seawater environments that doesn't incorporate steel reinforcement. Another option is to employ corrosion-resistant materials, such as fiber-reinforced polymers (FRP), in place of traditional steel reinforcement.

The possibility of using seawater for mixing concrete holds significant appeal. Studies suggest past success with seawater concrete, particularly in coastal regions like Southern California and Florida. This approach could offer environmental and economic benefits by reducing reliance on fresh water. This study investigated the effect of seawater on concrete strength, using Ordinary Portland Cement (OPC). While seawater can be an attractive alternative for mixing or curing concrete which alters the rate of strength gain. Compared to concrete specimens prepared and cured with fresh water, those using seawater exhibited a strength reduction of approximately 15% at 90 days.

The possibilities of using seawater in concrete has been investigated which indicated that it is a key consideration lies in its potential application. Studies suggest that seawater might be more suitable for unreinforced concrete and mortar, which constitute a significant portion (around 55%) of cement-based construction materials. Examples include bricklaying mortar, renders, and other non-structural elements. Studies investigating the viability of seawater concrete often raise concerns about its long-term performance. However, real-world examples offer encouraging evidence. Inspections of several unreinforced concrete structures along the coasts of Los Angeles and Florida, constructed using seawater for mixing and curing, have revealed no significant signs of degradation.

Seawater offers an attractive alternative for mixing concrete that shows a trade-off in strength compared to fresh water. However, this potential drawback might be addressed through the use of Glass Fiber Reinforced Polymer (GFRP). Reinforcement GFRP exhibits significant promise as a replacement for traditional steel rebar in chloride-rich environments like marine structures.

To unlock the broader application of concrete mixed with seawater, a comprehensive understanding of its behavior when combined with embedded GFRP bars is crucial. While extensive research exists on the durability of GFRP bars themselves, less is known about the long-term performance of GFRP-reinforced concrete structures exposed to marine environments.

On the other hand, ferro-cement beams have gained renewed interest as a construction material. The American Concrete Institute (ACI) Committee 549 has a long-standing definition established in 1971. According to ACI, ferrocement is a type of reinforced concrete typically constructed using a mortar matrix of hydraulic cement. This mortar is reinforced with closely spaced layers of fine wire mesh. The mesh can be metallic or composed of other suitable materials. Importantly, the fineness and composition of the mortar matrix should be compatible with the size and spacing of the reinforcing mesh to ensure proper encapsulation. The mortar matrix may also incorporate discontinuous fibers for additional reinforcement.

The influence of steel mesh type and the number of mesh layers on the performance of U-shaped ferrocement formwork beams has been investigated. The results revealed that these beams exhibited superior performance, characterized by increased ultimate and serviceability load capacity, improved crack control, enhanced ductility, and greater energy absorption. These findings align with similar observations reported by Shaheen and Eltehawy. Pardhe Bhattarai and Niti Bhattarai experimentally investigated the flexural behavior of solid and hollow

reinforced concrete beams. Six beams, each measuring 200mm x 300mm x 2300mm, were tested. Two beams were solid, while the remaining four had a longitudinal circular hollow section positioned below the calculated neutral axis. M30 grade concrete was used for all specimens. The beams were subjected to gradually increasing two-point loading, and a Linear Variable Displacement Transducer (LVDT) was employed to measure the resulting deflection. It can be concluded that the flexural behavior of the hollow-core beams closely resembled that of conventional reinforced concrete beams.

Desayi and El-Kholy investigated the stress-strain behavior of lightweight fiber-reinforced ferrocement specimens under uniaxial tension. It is revealed that the inclusion of fibers in the ferrocement specimens resulted in failure by a single dominant crack. This suggests that fiber-reinforced ferrocement members in tension behave more like a homogenous material, in contrast to specimens made solely of ferrocement.

Experimental testing showed that jute fiber reinforcement significantly improved the impact resistance of 500x500x50 mm ferrocement slabs, especially using a 50 mm crisscross pattern. This configuration increased first crack, slight separation, and full perforation loads by 722.58%, 232.26%, and 206.18%, respectively.

This study investigates the structural behavior of ferrocement beams constructed using seawater, aiming to replace traditional concrete beams. The research also explores the potential of seawater concrete as a sustainable alternative to freshwater concrete, focusing on its load-bearing capacity and crack resistance.

2. Materials and Methods

2.1 Materials

The experimental work employed Sulfate Resistance Cement (CEMI-42.5N) sourced from Al Tameer Cement, Giza, Egypt. This cement type is specifically designed for concrete exposed to severe sulfate attack, typically found in soils or groundwater with high sulfate content. The cement possesses a low Tricalcium Aluminate (C3A) content, generally below 5%. Natural siliceous sand was used as the fine aggregate. Two water sources were utilized: potable tap water and seawater sourced from the Red Sea in Ain-Sokhna, Egypt. Commercial-grade silica fume was obtained from Sika Company, Cairo, Egypt. Fiber mesh (e300) was procured from Geosegypt Company, Cairo, Egypt.

2.2 Method

Mix design

Six specimens, one control ferrocement beam with fresh water in concrete mix and three ferrocement beam with sea water in concrete mix were prepared and cast in the laboratory of Resistance and Testing of Materials at Housing and Building National Research Center (HBRC), Cairo, Egypt. All specimens were reinforced with fiberglass bars using 2Φ10 bars in the upper layer and 4Φ10 bars in the lower layer, in addition to a single layer of fiberglass mesh. The specimens had identical dimensions of 150×300×1600 mm with virous types of Mixing water ratio as shown in Fig. 1. The specimens were loaded in flexure under a two-point loading system with a simply supporting conditions up to failure as explained in Table 1.

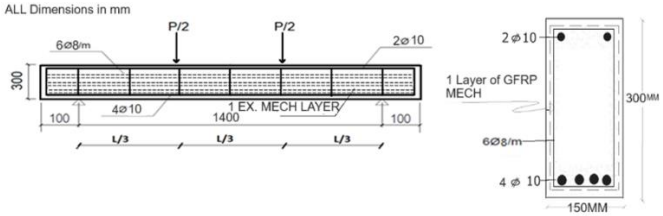

Fig. 1 Reinforcement and dimensions of tested specimens.

Table 1. Details of different groups of the mix.

Group	Beam	% Sea Water (Mixing)	% Sea Water (Curing)	Parameter
1	B1	0	0	- Control
2	B2	30	0	- Percentage of Sea Water Mixing
	B3	50	0	
	B4	100	0	
3	B5	100	50	- Percentage of sea water in Curing
	B6	100	100	- Percentage of Sea Water Mixing

The concrete mortar used for ferro-cement beams was designed to get an ultimate compressive Strength at 28-days age of (350 kg/cm2), 35 MPa. The mix properties for mortar matrix were chosen based on the (ACI committee 549 report: 1988 [1]). The matrix of ferro cement is mortar that consists of cement, sand, water and optionally an admixture Portland cement, fine grained sand, sea water and GFRP meshes. In mortar production, cement type will depend on source of sea water and the properties of sand, cement. Admixture was used as mortar super plasticizer to ensure the workability as shown in Table 2. Thus, the mortar was easily placed in molds despite the small aperture of square wire mesh.

Table 2. Mortar mix quantities.

MIX Design	Cement (kg/m³)	Sand (kg/m³)	Water (kg/m³)	Super plasticizer (kg/m³)	Silica fume (kg/m³)	Fibers (kg/m³)
Ratio from cement weight	1	2.2	0.4	0.01	0.1	0.0024
M1	626.4	1392	243.6	10.44	69.6	1.5

Preparation and Casting

For casting samples, wooden molds were used with the appropriate dimensions as shown in Fig. 2. The reinforcing fiber glass and fiber glass mesh were prepared outside the wooden mold with the required dimensions and details. It is worth mentioning that the concrete was cast after mixing for a period of between 10 and 12 minutes.

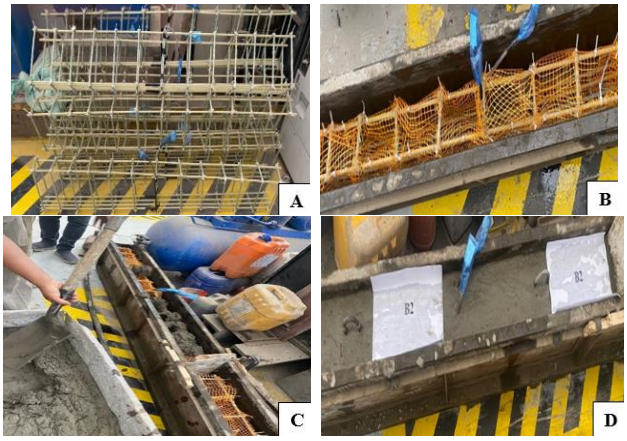

Fig. 2 Preparation and casting prosses.

Test Setup

The testing of RC beam specimens in flexure was conducted after 365 days of curing. All beams were painted with white plastic paint to help in crack detection during the testing process. The load was applied using the universal testing machine of capacity 200 kN in uniform ramping increments up to failure as shown in Fig. 3. The mid-span deflection was continually recorded using a linear variable displacement transducer (LVDT) placed under the center point of beam specimens, as shown in Fig. 3. At each load stage, the readings of deflection and strains were recorded automatically using a data logger connected to a computer

The crack pattern was also tracked and marked at each load stage. General structural behavior of the beam specimens was carefully observed during the load application. The failure load is identified when excessive cracking occurs at the bottom, the applied load drops, and the deflection increases. The trial mixes were prepared based on previous research, as shown in Table 3. The cubic specimens were cast using the same concrete mix as the 6 beam samples. Compression tests on the cubic specimens were conducted on the same days as the beam samples, with some cubes tested after 7 days and the remaining cubes tested after 365 days. The number of cubic specimens was equal to the number of beam specimens.

Table 3. Compression test results.

Period (days)		7 days	365 days
		Peak compressive strength (MPa)	
Cubic specimen no.	1	29.1	43.17
	2	29.3	44.7
	3	29.6	45.17
	4	30.1	46.20
	5	30.2	47.70
	6	30.5	49.2

Fig. 3 Test setup configurations.

3. Results and Discussion

3.1 Materials characterization

The main compounds, chemical constituents, physical characteristics, specific weight, bulk density, soundness and alkali equivalent of the used sulfate resistance cement (cemi-42.5 n) have been determined as presented in Table 4.

Table 4. Physical properties of Sulphate Resist Cement.

Test Description	Test Result	Specification Limits
Percentage of water to give a paste of standard consistency, w/c %	45 %	
Setting time (Vicat test) - Initial - Final	Hr: min 1: 30 4: 45	Not less than 45 min Not more than 10 hr
Soundness of cement (Le Chatelier test)	5 mm	Not more than 10 mm
Fineness of cement, Percentage retained on the Standard 0.09 mm sieve by weight	8 %	Not more than 10 %
Compressive strength of Morta 7x7 cm cubes - 3 days - 4 days	195 kg/cm^2 290 kg/cm^2	Not less than 185 kg/cm^2 Not less than 275 kg/cm^2

The natural siliceous sand used as fine aggregate is clean and nearly impurity-free, with a specific gravity of 2.6 and a modulus of fineness of 2.91. It is clear that the sand's characteristics are in agreement with E.S.S. 1109/2008. The characteristics of the sand used are shown in Table 5, and the grading of the sand is shown in Table 6 and Fig. 4.

Table 5. Properties of fine aggregate used.

Property	Test results for Sand
Specific Gravity (S.S.D)	2.6
Unit Weight	1.7
Fineness Modulus	2.91
Clay, Silt, and Fine Dust	2% (by weight)
Percent of Chloride	0.03 (by weight)

Table 6. Sieve analysis of the used fine aggregates.

Sieve Diameter (mm)	4.75	2.36	1.18	0.6	0.3	0.15
% Passing	100	92.8	82.6	37.7	9.50	0
% Passing (E.S.S. 1109/2008) (Medium Zone)	100	60-100	30-90	15-45	5-40	0

The two types of mixing water were analyzed chemically using inductively coupled plasma mass spectrometry (ICP-MS) to determine chlorides, sulfates, alkalinity, total dissolved solids, and pH (at 25°C). These measurements were compared according to the Egyptian specifications as shown in Table 7.

The used silica fume is typically a gray-colored powder that resembles Portland cement or fly ashes. It has a powder form and is a light grey color, bulk density 300 kg/m3 and density 350 kg/m3. Silica fume is described by the American Concrete Institute (ACI) as "very fine non-crystalline silica produced in electrical furnaces as a by-product of the production of elemental silicon or alloys containing silicon" (ACI 116R). Condensed silica fume was utilized as a partial replacement for cement in mortar so that it can increase the strength and permeability of the mortar matrix.

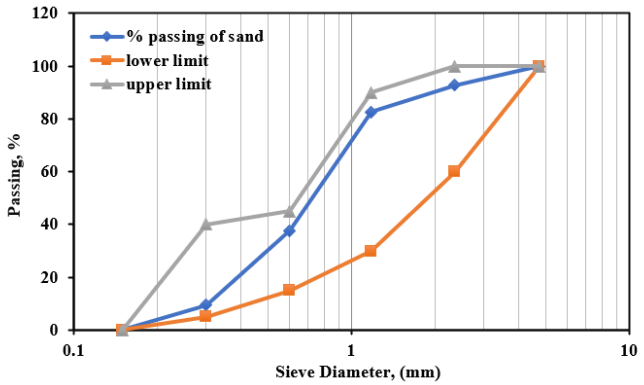

Fig. 4 Grading curve of the used sand.

The fiber mesh used in the current study with specific gravity 0.91, melting point 324°F (162°C), Ignition Point 1100°F (593°C) and fiber mesh e300. Fibers are frequently used to avoid cracking, which is a result of drying shrinkage and heat expansion/contraction. Additionally, it was utilized to provide fibrillated toughness and residual strength to concrete, increase impact resistance, shatter resistance, and abrasion resistance.

A high-range water-reducing (HRWR) admixture (Sikament 163 M) was used to produce concrete with a high workability with 1.2 kg/lit density. The technical characteristics of the admixture utilized, according to the manufacturer.

ARMASTEK® _Russia produced the GFRP bars used in this study and were contrived by the pultrusion method of E-glass fibers impregnated in modified vinyl ester resin. A 10-mm rebar glass fiber reinforced polymer (GFRB) manufactured by Russian Company Armastek was used. The reported laboratory mechanical properties for the average ultimate tensile strength were 1035 MPa with maximum strain of 0.0245 in accordance with ASTM Standard (ASTM D7205-06).

Table 7. Chemical characterization of the used mixing water.

Test	Results (ppm)	
	Fresh water	Seawater
Chloride (Cl^-)	52	25000
Sulfate (SO_4^{-2})	56.28	4357
Total dissolved solids (TDS)	342.54	51285
pH (at 25 °C)	7.62	7.38
Turbidity	.51	1.38
HCO_3	140	130

3.2 Mechanical Properties

The test results listed in Table 8 summarize the obtained experimental results for each specimen as well as the ultimate failure load, the first crack load, ductility ratio, and energy absorption for each group. Ductility ratio is defined as the ratio between the mid-span deflection at ultimate load to that at the first crack load, while the energy absorption is defined as the area under the load-deflection curve. The load-deflection curves of tested specimens are shown in Fig. 5. The load-deflection relationship can be divided into three regions: a) linear relationship up to the first cracking of concrete; b) transition region, where the relation deviated from linearity due to continuous cracking of the beam and c) large plastic deformation.

Table 8. Comparison of flexural behavior results.

Group	Beam	First Crack Load (Pcr)		Ultimate Load (Pu)		Deflection at First Crack (δcr)		Deflection at Ultimate (δu)		Energy Absorption Capacity	
		Measured (kN)	Relative (%)	Measured (kN)	Relative (%)	Measured (mm)	Relative (%)	Measured (mm)	Relative (%)	Measured (kN.mm)	Relative (%)
1	B1	36.10	100%	187.11	100%	0.99	100%	16.11	100%	1,920.79	100%
2	B2	36.55	101%	194.27	104%	0.87	88%	18.22	113%	2,224.84	116%
	B3	47.80	132%	220.10	118%	0.90	92%	21.50	133%	3,270.00	170%
	B4	45.07	125%	223.82	120%	1.76	178%	24.15	150%	3,508.36	183%
3	B5	49.32	137%	233.40	125%	1.18	120%	27.17	169%	4,131.80	215%
	B6	57.30	159%	275.80	147%	2.01	203%	34.67	215%	6,762.79	352%

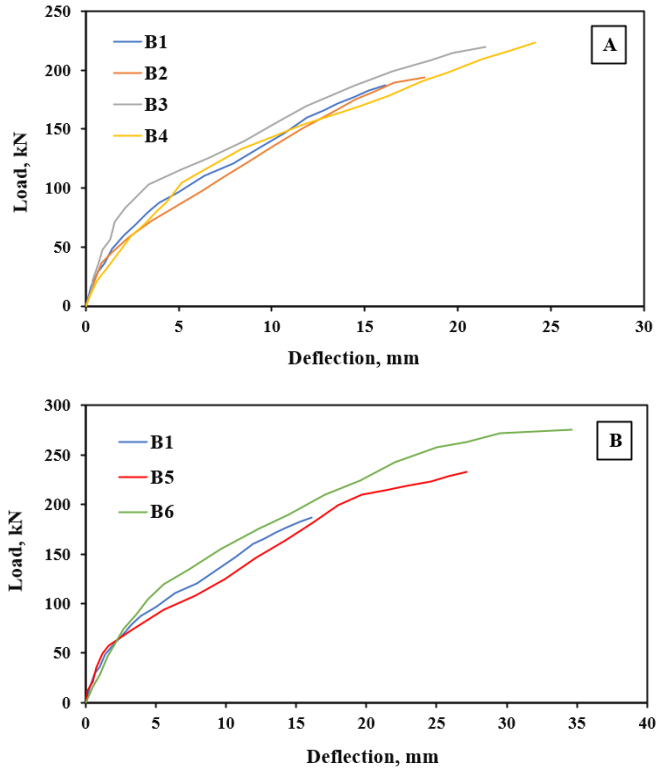

Fig. 5 Load-Deflection curve of tested specimens where A) for group one and group two, B) for group one and group three.

The measured load-deflection response curves of the tested specimens are summarized in Figures 5 and 6. It is clear that the ultimate load of all beams in group two was increased by the addition of seawater in the concrete mix by about 4% and 18%. Group three beams achieved the highest ultimate load, with increases of about 20%, 25%, and 47% compared to the control beam and group two, respectively, when cured with seawater.

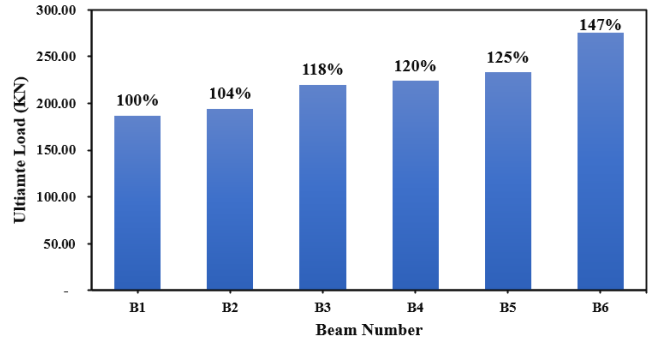

Fig. 6 Ultimate loads values of all tested beams.

Figure 7 presents the load-strain relationships for the top middle compression zone of all tested beams. A linear elastic response was observed prior to initial cracking. The control beam (B1) exhibited an average compression strain of -0.001914. Seawater-mixed beams (B2, B3, and B4) demonstrated slightly increased strains, with approximately 2%, 3%, and 3% higher values, respectively. Seawater-mixed and cured beams (B5 and B6) exhibited a more pronounced increase in strain, with approximately 5% higher values compared to the control beam.

Energy absorption, a measure of a beam's ability to absorb energy before breaking, is calculated as the shaded area under the load-deflection curve. The area under the curve was calculated using a computer program (BASIC language). The ultimate load energy absorbed was calculated using Eq. (1)

$$\text{Ultimate Load Energy Absorbed} = \int_0^{\Delta u} f(\Delta)\, d\Delta \qquad (1)$$

Where f (Δ) is the equation of the load-deflection curve, and Δu is the mid-span deflection at failure load.as shown in Fig.8.A larger shaded area indicates a higher capacity for energy absorption.

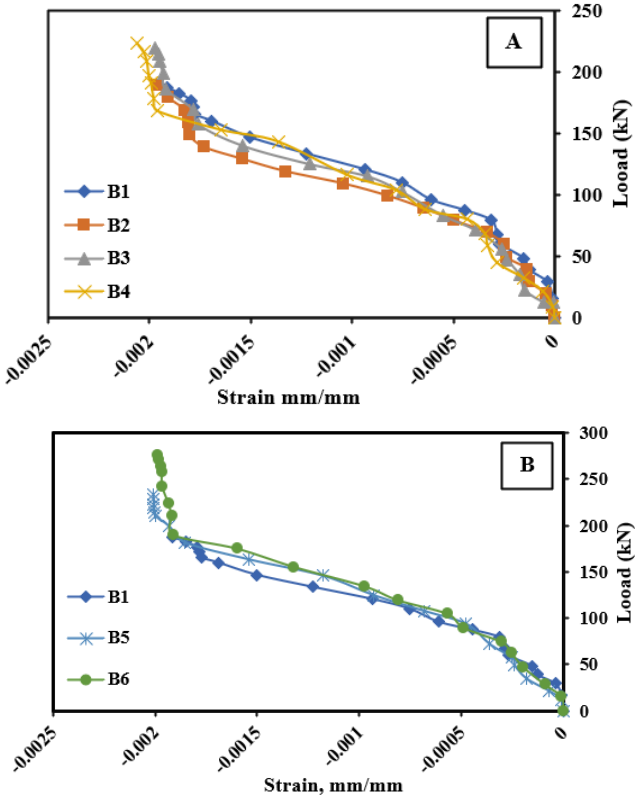

Fig. 7 The load-strain curve of tested specimens where A) for group one and group two, B) for group one and group three.

This graphical representation highlights that a larger enclosed area signifies a greater capacity for the beam to absorb energy (refer to Table 8 for detailed data) , the analysis revealed that beam B6 within Group three exhibited the superior performance in terms of energy absorption compared to all other tested beams ,this indicates a potential design advantage for beams in group four, warranting further investigation into the specific characteristics that contribute to this enhanced energy absorption. Furthermore, the experiment evaluated the relative energy absorption of different beam groups compared to a control beam the observations are summarized as group two 16% increase in energy absorption was observed reaching a value of 83%, group three demonstrated the most significant improvement, with a remarkable 115% increase resulting in a very high energy absorption of 252%.

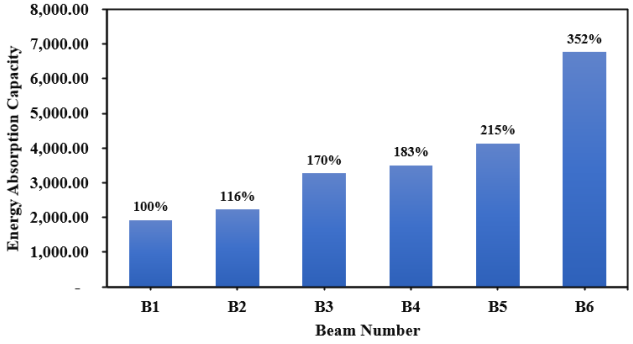

Fig. 8 Energy absorption capacity of all tested beams.

Fig. 9 illustrates the cracking patterns observed in all tested beam specimens. In the control specimens, initial cracks appeared at mid-span. With increasing applied load, these cracks propagated rapidly from the tension side towards the compression side, extending along the entire beam span. For Groups two and three, the first crack also initiated near mid-span, with the first crack load varying depending on the seawater percentage as detailed in Table 8. As the load increased further, new cracks developed on either side of the first crack, while the first crack itself propagated vertically. With additional load increments, new cracks formed, and existing cracks propagated in a near-diagonal direction. This pattern of crack development continued until beam failure. The number of cracks observed varied depending on the seawater percentage used in each specimen. It is important to note that all beam specimens exhibited shear compression failure due to the use of the minimum required bending reinforcement ratio.

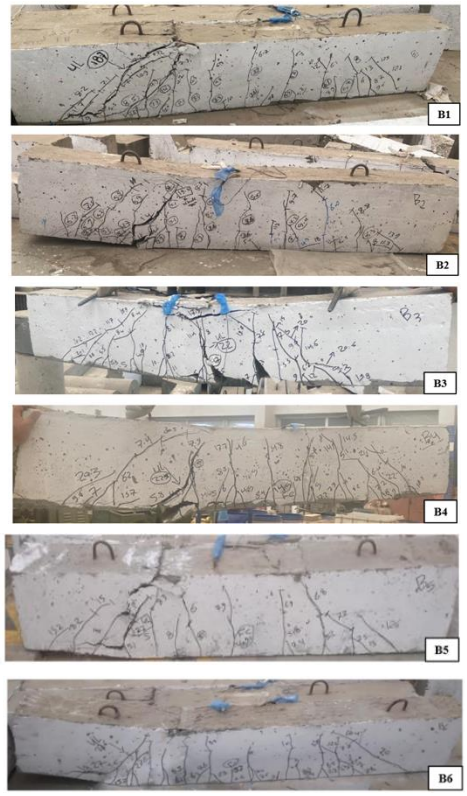

Fig. 9 Ultimate loads values of all tested beams.

4. Conclusions

Based on the results and observations of the experimental study presented in this paper. the following conclusions can be drawn:

(1) Comparing Groups 2 and 3, using seawater in both the mix and cure appears to significantly enhance performance compared to just using it in the mix. This suggests seawater interaction throughout the curing process plays a role in improving the properties of the ferrocement beams.

(2) Group 3 (100% seawater) consistently outperformed other groups in both ultimate load and energy absorption.

(3) The significant improvement in energy absorption across all beams using seawater in mixing and curing resulted in beams with higher energy absorption capacity.

(4) Greater exposure to seawater results in a higher number of cracks appearing in each test sample.

References

WHO, W.H.O. (2000). Global Water Supply and Sanitation Assessment 2000 Report. World Health Organization (WHO) and the United Nations Children's Fund (UNICEF), Geneva.

Meyer, C. (2009). "The Greening of the Concrete Industry." Cement and Concrete Composites, Elsevier Ltd, 31(8), 601–605. https://doi.org/10.1016/j.cemconcomp.2008.12.010

Otsuki, N., Furuya, D., Saito, T., & Tadokoro, Y. (2011). "Possibility of Sea Water as Mixing Water in Concrete." 36th Conference on Our World in Concrete & Structures, Singapore. http://cipremier.com/100036021

Metwally, M.H.S., Genidi, M.M.M., Ibrahim, A.H., & Ebead, U.A.A. (2022). "Experimental Study on Performance of Seawater Concrete Beams." International Journal of Civil and Structural Engineering Research. https://doi.org/10.1007/978-3-031-70145-0_88

Otsuki, N., Saito, T., & Tadokoro, Y. (2012). "Possibility of Sea Water as Mixing Water in Concrete." Journal of Civil Engineering and Architecture, ISSN 1934-7359, Vol. 6, No. 10, pp. 1273–1279, USA. http://cipremier.com/100036021

Gleick, P.H. (1993). Water in Crisis (Vol. 100). New York: Oxford University Press.

Younis, A., Ebead, U., & Nanni, A. (2017). "A Perspective on Seawater/FRP Reinforcement in Concrete Structures." ISEC 2017.

Otsuki, N., Saito, T., & Tadokoro, Y. (2012). "Possibility of Sea Water as Mixing Water in Concrete." Journal of Civil Engineering and Architecture, 6(11). https://doi.org/10.17265/1934-7359/2012.10.00.

Guo, Q., Chen, L., Zhao, H., Admilson, J., & Zhang, W. (2018). "The Effect of Mixing and Curing Seawater on Concrete Strength at Different Ages." MATEC Web of Conferences, Vol. 142, p. 02004. EDP Sciences. https://doi.org/10.1051/matecconf/201814202004

Scrivener, K.L., John, V.M., & Gartner, E.M. (2018). "Eco-efficient Cements: Potential Economically Viable Solutions for a Low-CO2 Cement-Based Materials Industry." Cement and Concrete Research. https://doi.org/10.1016/j.cemconres.2018.03.015

Hadley, H. (1935). "Letter to the Editor," Engineering News-Record, 716–717.

ACI (1940). "Job Problems and Practice," American Concrete Institute, 313–314. https://doi.org/10.1520/STP35643S

Nanni, A., De Luca, A., & Zadeh, H.J. (2014). FRP Reinforced Concrete Structures: Theory, Design, and Practice. Boca Raton, FL: CRC Press. https://hdl.handle.net/11588/586134

Zhou, J., Chen, X., & Chen, S. (2012). "Effect of Different Environments on Bond Strength of Glass Fiber-Reinforced Polymer and Steel Reinforcing Bars." KSCE Journal of Civil Engineering, 16(6), 994–1002. https://doi.org/10.1007/s12205-012-1462-3

Chen, Y., et al. (2007). "Accelerated Aging Tests for Evaluations of Durability Performance of FRP Reinforcing Bars for Concrete Structures." Composite Structures, 78(1), 101–111. https://doi.org/10.1016/j.compstruct.2005.08.015

Hao, Q., et al. (2009). "Bond Strength of Glass Fiber Reinforced Polymer Ribbed Rebars in Normal Strength Concrete." Construction and Building Materials, 23(2), 865–871. https://doi.org/10.1016/j.conbuildmat.2008.04.011

Bank, L.C., Puterman, M., & Katz, A. (1998). "The Effect of Material Degradation on Bond Properties of Fiber Reinforced Plastic Reinforcing Bars in Concrete." ACI Materials Journal, 95(3), 232–243. https://doi.org/10.14359/367

Robert, M., & Benmokrane, B. (2010). "Effect of Aging on Bond of GFRP Bars Embedded in Concrete." Cement and Concrete Composites, 32(6), 461–467. https://doi.org/10.1016/j.cemconcomp.2010.02.010

Abbasi, A., & Hogg, P.J. (2005). "Temperature and Environmental Effects on Glass Fibre Rebar: Modulus, Strength, and Interfacial Bond Strength with Concrete." Composites Part B: Engineering, 36(5), 394–404. https://doi.org/10.1016/j.compositesb.2005.01.006

Bank, L.C., Puterman, M., & Katz, A. (1998). "The Effect of Material Degradation on Bond Properties of FRP Reinforcing Bars in Concrete." ACI Materials Journal, 95, 232–243. https://doi.org/10.14359/367

ACI Committee 549. (1997). State-of-the-Art Report on Ferrocement. ACI 549R-97, 1–26.

Abd ElMohimen, H.M.R. (2005). "Structural Behaviour of Ribbed Ferrocement Plate." B.Sc. Thesis submitted to Menoufia University, Egypt.

Channi, A.S. (2009). "Effect of Percentage of Reinforcement on Beams Retrofitted with Ferrocement Jacketing." Thapar University Patiala-147004.

Fahmy, E.H., Shaheen, Y.B.I., Abdelnaby, A.M., & Zeid, M.N.A. (2014). "Applying the Ferrocement Concept in Construction of Concrete Beams Incorporating Reinforced Mortar Permanent Forms." Int. J. Concr. Struct. Mater., 8(1), 83–97. https://doi.org/10.1007/s40069-013-0062-z.

Shaheen, Y.B.I., & Eltehawy, E.A. (2017). "Structural Behaviour of Ferrocement Channel Slabs for Low-Cost Housing." Challenge J. Concr. Res. Lett., 8(2), 48–64. https://doi.org/10.20528/cjcrl.2017.02.002

Bhattarai, B., & Bhattarai, N. (2017). "Experimental Study on Flexural Behavior of Reinforced Solid and Hollow Concrete Beams." International Journal of Engineering Research and Advanced Technology, 3(11), 1–8. http://dx.doi.org/10.7324/IJERAT.2017.3149

Desayi, P., & El-Kholy, S.A. (1991). "Lightweight Fibre-Reinforced Ferrocement in Tension." Cem. Concr. Compos., 13, 37–48. https://doi.org/10.1016/0958-9465(91)90045-I

Salih, Y.A., Sabeeh, N.N., Yass, M.F., Ahmed, A.S., Abdulla, A.I. (2020). "Behavior of Ferrocement Slabs Strengthened with Jute Fibers under Impact Load." International Review of Civil Engineering, 11(2), 66–72. https://doi.org/10.15866/irece.v11i2.17322

Disclaimer